

Insights into the Mechanism of Cumene Peroxidation using Supported Gold and Silver Nanoparticles

Charles O'Neil Crites, Geniece L. Hallett-Tapley, Mathieu Frenette, Maria Gonzalez-Bejar, Jose Carlos Netto-Ferreira, and Juan C. Scaiano

ACS Catal., **Just Accepted Manuscript** • DOI: 10.1021/cs400337w • Publication Date (Web): 22 Jul 2013

Downloaded from <http://pubs.acs.org> on July 29, 2013

Just Accepted

"Just Accepted" manuscripts have been peer-reviewed and accepted for publication. They are posted online prior to technical editing, formatting for publication and author proofing. The American Chemical Society provides "Just Accepted" as a free service to the research community to expedite the dissemination of scientific material as soon as possible after acceptance. "Just Accepted" manuscripts appear in full in PDF format accompanied by an HTML abstract. "Just Accepted" manuscripts have been fully peer reviewed, but should not be considered the official version of record. They are accessible to all readers and citable by the Digital Object Identifier (DOI®). "Just Accepted" is an optional service offered to authors. Therefore, the "Just Accepted" Web site may not include all articles that will be published in the journal. After a manuscript is technically edited and formatted, it will be removed from the "Just Accepted" Web site and published as an ASAP article. Note that technical editing may introduce minor changes to the manuscript text and/or graphics which could affect content, and all legal disclaimers and ethical guidelines that apply to the journal pertain. ACS cannot be held responsible for errors or consequences arising from the use of information contained in these "Just Accepted" manuscripts.



Insights into the Mechanism of Cumene Peroxidation using Supported Gold and Silver Nanoparticles

Charles-Oneil L. Crites,^a Geniece L. Hallett-Tapley,^a Mathieu Frenette,^a María González-Béjar,^{a,b} J.C. Netto-Ferreira^{a,c*} and J. C. Scaiano^{a*}

^a Department of Chemistry and Centre for Catalysis Research and Innovation, University of Ottawa, 10 Marie Curie, Ottawa K1N 6N5, Canada

^b Instituto de Ciencia Molecular, Departamento de Química Orgánica, Universidad de Valencia, C/Catedrático José Beltrán, 2, 46980, Paterna, Valencia, Spain

^c Departamento de Química, Universidade Federal Rural do Rio de Janeiro, Seropédica, 23851-970, Rio de Janeiro, Brazil

ABSTRACT: Due to the considerable industrial implications, an in-depth study of cumene peroxidation using supported gold and silver nanoparticles was carried out to gain more insight into the mechanism of this reaction. Supported gold nanoparticles were found to efficiently catalyze the decomposition of cumene hydroperoxide with a selectivity of 25% at 80°C when using gold supported on hydrotalcite (AuNP@HT) and 2-phenyl-2-propanol (i.e., cumyl alcohol) was the main product. Further, silver nanoparticles supported on hydrotalcite (AgNP@HT) converted cumene to cumene hydroperoxide at 80°C with 80% selectivity. Both benchtop and oxygen-uptake experiments were used to probe the reaction mechanism and suggest that formation of a peroxy radical-nanoparticle adduct is an important step in the peroxidation pathway and may be directly involved in the formation of the major cumyl alcohol product.

KEYWORDS: oxidation; free radicals; heterogeneous catalysis; hydrotalcite; nanotechnology; Hock rearrangement

INTRODUCTION

Oxidation reactions are one of the most fundamental reactions at the industrial level. Notably, free-radical reactions are used to synthesize several chemicals, including cyclohexane hydroperoxide, ethylbenzene hydroperoxide, and cumene hydroperoxide. These hydroperoxides are important intermediates in several industrial processes.¹ In particular, cumene hydroperoxide accounts for the vast majority of the world production of acetone and phenol. Considerable efforts have focused on the catalytic formation of hydroperoxides. Ethylbenzene hydroperoxide is a key intermediate in the Hock process, commonly formed by the metal salt catalyzed free-radical oxidation of tetraline in the 1950's and 60's.^{2, 3} Later, heterogeneous materials, notably MnO₂ and Cu₂O,⁴ were used in the free-radical oxidation of cumene. More recently, nanostructures have been investigated as potential alternative catalysts in hydroperoxidations. One of the more recent examples involves ethylbenzene oxidation using NiAl hydrotalcite catalysts, also thought to proceed *via* a free-radical mechanism.⁵ In many cases the catalytic process can be viewed as a desirable perturbation of the well-established autoxidation of reactions 1-4.

Initiation : production of R•, ROO• or RO• (1)

Propagation: R• + O₂ → ROO• (2)



The initiation (1), the propagation (2 and 3) and the termination (4) are steps that occur in a typical free radical chain reaction.

Although formation of hydroperoxides through the use of a variety of catalysts has been demonstrated,⁶ a major disadvantage that still remains relates to the instability of hydroperoxides in the presence of the catalyst.⁷ Typically, the hydroperoxide will decompose into the corresponding alcohol. This pathway can sometimes be useful, as in the case of cyclohexane oxidation to cyclohexanol,⁸⁻¹¹ an important step in the formation of caprolactam, the major precursor for the synthesis of Nylon-6.

Also of considerable importance is the Hock rearrangement from cumene hydroperoxide to phenol and acetone, highly sought-after in the chemical industry.¹² However, several studies examining the formation of cumene hydroperoxide using silver nanoparticles on Al₂O₃,¹³ as well as copper and copper oxide nanoparticles¹⁴ on MgO,¹⁵ have shown that the undesired cumyl alcohol was obtained in significant yields. Further studies by Lloyd *et al.*¹⁶ using supported gold nanoparticles have demonstrated the importance of the support towards hydroperoxide stability. Silver nanoparticles (AgNP) have been shown to catalyze the peroxidation of cumene, even though the influence of the support in these reactions

was not conclusive.⁶ More so, the work of Ham *et al.*¹³ demonstrates that AgNP, under oxygen, do not degrade cumene hydroperoxide, but still catalyze cumene peroxidation.

From the literature, it is evident that some supported nanoparticle catalysts strongly influence the stability of hydroperoxides, as well as that of common radical initiators.^{17, 18} Due to the sheer importance of cumene hydroperoxide, this contribution will focus mainly on this intermediate and is aimed at examining the use of potential heterogeneous nanoparticle catalysts, specifically supported AuNP and AgNP, not only to maximize cumene hydroperoxide production, but also reduce the yield of the cumyl alcohol by-product, formed *via* hydroperoxide degradation.

Clearly, some catalysts and their supports can influence the stability of the hydroperoxide, a product of the reaction, but also play an important role as a radical initiator. This work was undertaken with two questions in mind:

Do typical oxidation catalysts induce the decomposition of typical oxidation initiators, in particular hydroperoxides?

Do oxidation catalysts influence in any way (catalysis or inhibition) the kinetics of the free-radical chain reaction that mediates oxidation?

To the best of our knowledge, these questions have not been addressed in any detail in earlier work, especially when considering supported AuNP; yet, we believe that understanding these issues is key to mechanistic proposals dealing with the catalytic oxidation of alkenes (leading to epoxides), as catalyst-induced initiator decomposition will have significant effects on both the kinetics and efficiency of such reactions. Most work was carried out at low conversions to reveal the early stages of the oxidation process. Clearly it would be impossible to address questions (i) and (ii) for all combinations examined in the literature. We simply aim at addressing these issues for some key systems, notably some widely employed supported gold nanoparticles, such as commercially available AuNP@TiO₂. This work also allows the opportunity to study the formation of cumene hydroperoxide, which is made *via* the auto-oxidation of cumene in a process that is not catalyzed in industry.¹⁹

EXPERIMENTAL

Reagents. Cumene, cumene hydroperoxide (CHP), (technical grade 80%, largely cumene impurity), cumyl alcohol (98 %; 2-phenyl-2-propanol), acetophenone (98 %), dicumyl peroxide (DCP) (97 %), 2,6-di-*tert*-butyl-4-methoxyphenol (95%, DBHA), *tert*-butyl hydroperoxide solution in H₂O (80%) and dodecane (99%), chlorobenzene (99.5%), hydrotalcite (HT), sodium borohydride (NaBH₄), tetrachloroauric acid (HAuCl₄•H₂O), silver nitrate, phenol, lipoic acid (99%) and optima grade acetonitrile were purchased from Sigma-Aldrich and used as received. TiO₂ P25 was a gift from Evonik Degussa. AUROLite™ 1% AuNP@TiO₂ was purchased from Strem Chemicals and was ground using a mortar and pestle prior to use. The average size of the AuNP was determined to be 2.3 nm by TEM (Figure S1). Optima grade heptane, 2-propanol and ammonia (28% in H₂O) were purchased from Fisher Chemicals and used as received. Millipore H₂O was deionized in house (18.2Ω at 25°C) and used in the synthesis of supported metal nanoparticles.

Instruments. The size of the metallic nanoparticles was determined using a JEM-2100F FETEM transmission electron microscope (TEM) from Jeol Ltd. Analysis of the reaction

mixture (cumyl alcohol, acetophenone and cumene hydroperoxide) was carried out using a normal phase Agilent 1100 HPLC (eluent 99:1 heptane:2-propanol). The amount of dicumyl peroxide was determined using a Waters HPLC fitted with a reverse phase C-18 silica column and employing an eluent mixture of 60:40 acetonitrile:water. Representative reverse and normal phase HPLC spectra are shown in Figures S4 to S6. Experiments requiring controlled gas flow used a Matheson flow meter.

Synthesis of supported gold nanoparticles on hydrotalcite (AuNP@HT). The procedure was adapted from previous work by Mitsudome *et al.*²⁰ 2 g of hydrotalcite were added to 60 mL of an aqueous solution of 1.8 mM HAuCl₄•H₂O. 0.09 mL of a 10% solution of NH₄OH was added after several minutes and the mixture was allowed to stir overnight. The supported Au³⁺ composite was filtered, washed with water, re-suspended in water and 10 mL of a 200 mM solution of sodium borohydride were added and allowed to react for two hours. Finally, the purple solid was filtered, washed with water and dried under ambient conditions. The theoretical loading was 1 % and the average nanoparticle size was determined to be 5.8 nm by TEM (see Figure 1 and S2).

Synthesis of supported silver nanoparticles on hydrotalcite (AgNP@HT). The procedure was adapted from previous work from Mitsudome and co-workers.²¹ 2 g of hydrotalcite were added to 60 mL of an aqueous solution of 2.9 mM silver nitrate. The solution was cooled using an ice bath and purged with nitrogen. After stirring for 4 hours, the Ag⁺/hydrotalcite composite was filtered, washed and re-suspended in water. Under a nitrogen atmosphere, 10 mL of a 200 mM solution of sodium borohydride were added to the slurry. The yellow solid was then filtered and washed with water and dried at ambient temperature. The theoretical loading was calculated to be 1% and the average nanoparticle size was determined to be 10 nm by TEM (see Figure 1 and S3).

Peroxidation of cumene under atmospheric conditions. In a 50 mL, two-neck round bottom flask, 200 mg of catalyst and 12 μl (0.05 mmol) of an aqueous solution of *tert*-butyl hydroperoxide were added to 20 mL of cumene and the reaction heated to 80 °C. This corresponds to 0.035% equivalents of initiator; note that conversions are low and that the reaction generates hydroperoxides that also act as initiators. An aliquot was taken from the reaction mixture every hour, centrifuged and subsequently analyzed HPLC. Control reactions were carried out using the support itself and in the absence of heterogeneous materials (*tert*-butyl hydroperoxide initiator only).

Peroxidation of cumene under oxygen saturated conditions. The experimental protocol is the same as used for the reactions under atmospheric conditions. However, oxygen was continuously bubbled into the solution using a Teflon needle in order to prevent contamination by iron. The oxygen flow was controlled using a flow regulator.

Decomposition of cumene hydroperoxide (CHP) in dodecane. In a 50 mL, two-neck flask, 200 mg of catalyst and 500 μl of an 80% solution of cumene hydroperoxide were added to 20 mL of dodecane and the reaction was heated to 80 °C. An aliquot was taken from the reaction mixture every hour, centrifuged and then analyzed *via* HPLC. Control reactions were also carried out as indicated in the procedure for the peroxidation of cumene under O₂.

Oxygen uptake experiments. The oxygen uptake apparatus was a gift from Prof. Ross Barclay of Mount Allison University (Sackville, NB). This system, built in-house, monitors small pressure differences between two samples (sensitivity

< 100 nmol O₂). Technical details of the design are presented elsewhere.^{22, 23} The amount of oxygen consumed was determined by measuring the change in the pressure difference between the reference and the reaction cell. Oxygen uptake experiments were carried out at 30°C due to technical limitations of the instrument.

The experiments were conducted as follows: 5 mL of cumene were added to the reference and reaction cells and then 12.6 mg of the catalyst of interest were added to the reaction cell. To initiate the reaction, 100 µL of a 176 mmol aqueous solution of *tert*-butyl hydroperoxide were added to the reaction cell. The rate of propagation is determined by graphical measurements and corresponds to the first derivative of the amount of oxygen produced with time.

Oxygen uptake experiments: Determining the rate of initiation (R_i)

The same general procedure described in the preceding section was used; however after measuring the rate of propagation, 100 µL of 8.0 mmol solution of 2,6-di-*tert*-butyl-4-methoxyphenol antioxidant were added in order to determine the inhibition period due to trapping of radical species. This inhibition period provides information about the rate of initiation, which corresponds to the rate at which free radicals are formed from non-radical precursors.²⁴

Recyclability Experiments

In a 50 mL, two-neck round bottom flask, 200 mg of catalyst and 12 µL (0.05 mmol) of an aqueous solution of *tert*-butyl hydroperoxide were added to 20 mL of cumene and the reaction heated to 80°C for a period of 8 hours. After reaction, the slurry was transferred to glass centrifuge tubes and centrifuged at 3000 rpm for 15 minutes. The catalyst was separated from the reaction mixture and washed three times using CH₃CN to remove any adsorbed organics from the composite surface.

Peroxidation Inhibition using 2,6-di-*tert*-butyl-4-methoxyphenol (DBHA) and AuNP Surface Functionalization using Lipoic Acid

In a 50 mL, two-neck round bottom flask, 100 mg of catalyst and 7 µL (0.025 mmol) of an aqueous solution of *tert*-butyl hydroperoxide were added to 10 mL of cumene and the reaction heated to 80°C for a period of 3 hours. An aliquot was taken every 30 minutes, centrifuged and subsequently analyzed by HPLC. Either 100 mg of 2,6-di-*tert*-butyl-4-methoxyphenol or 5 mg of lipoic acid were added after 1 hour to observe the effects on the overall product yields.

RESULTS

The TEM image of AuNP@HT, shown in Figure 1a, illustrates an average NP size of 5.8 ± 2.7 nm. Likewise, Figure 1b presents a representative TEM image for AgNP@HT and average particle sizes of 10 ± 3.2 nm. The corresponding size distribution histograms are presented in Figures S2 to S3. Additionally, TEM of the commercial AuNP@TiO₂ can be seen in Figure S1.

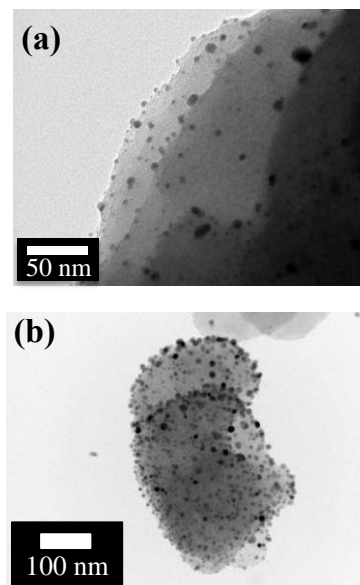


Figure 1. Representative TEM images of (a) AuNP@HT and (b) AgNP@HT

Commercial AuNP@TiO₂ as a catalyst for cumene peroxidation. Our initial goal was to study cumene peroxidation using commercially available AuNP supported on TiO₂ in the presence of a *tert*-butyl hydroperoxide initiator. As illustrated in Figure 2, when the reaction is performed in the absence of nanoparticle catalyst, a 1.0 % yield of cumene hydroperoxide (CHP) was obtained after 24 hours of reaction. When the support alone (TiO₂) was used, minimal yields of cumene hydroperoxide were observed. On the other hand, using commercial AuNP@TiO₂ as the catalyst, yields of 3.8 % for cumyl alcohol and 1.0 % for cumene hydroperoxide were obtained. The different product distributions obtained when using the support alone and the nanomaterial indicate that TiO₂ alone is not capable of cumene hydroperoxide decomposition into cumyl alcohol via a free-radical pathway.²⁵

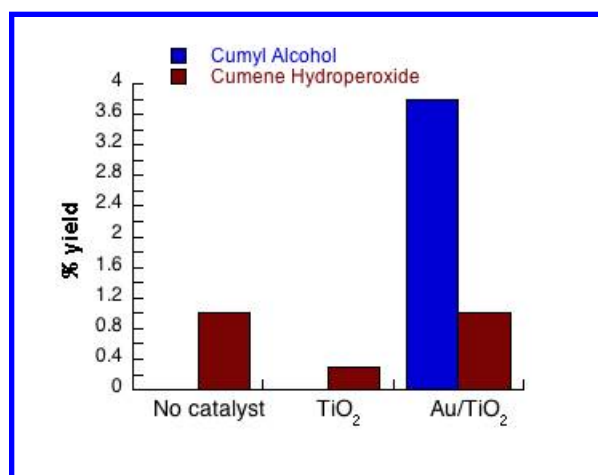


Figure 2. Bar graph illustrating the yield of cumyl alcohol and cumene hydroperoxide after 24 hours when using no catalyst, TiO₂ and commercial AuNP@TiO₂ at 80°C and *tert*-butyl hydroperoxide as an initiator.

The reaction kinetics using commercial AuNP@TiO₂ (Figure 3) monitored over 8 hours clearly shows that cumene hydroperoxide

eroxide is not detected before three hours of reaction and that cumyl alcohol is the major product obtained.

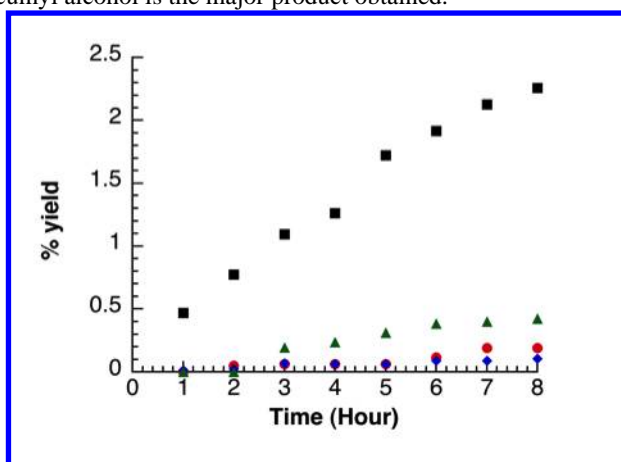
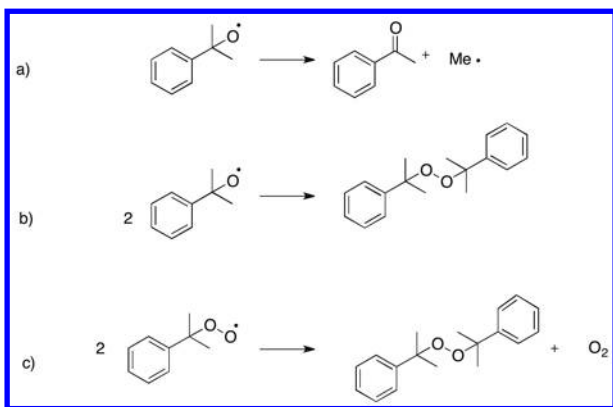


Figure 3. Percent yield of cumyl alcohol (■), CHP (●), acetophenone (◆) and DCP (▲) obtained for the peroxidation of cumene using commercial AuNP@TiO₂ at 80°C over 8 hours.

Other secondary products were obtained in small quantity when commercial AuNP@TiO₂ was used as a peroxidation catalyst (Figure 3). Acetophenone was formed from a secondary radical pathway involving β -scission of the cumyloxy radical, while dicumyl peroxide (DCP) resulted from the recombination of two cumyl peroxy radicals or two cumyloxy radicals (Scheme 1). Notably, cumene peroxidation control experiments run in the absence of catalyst or using TiO₂ alone yielded only trace amounts of product (Figures S7 and S8).



Scheme 1. Formation of secondary products for cumene peroxidation using commercial AuNP@TiO₂: a) formation of acetophenone via β -scission, b) formation of DCP via radical recombination of two cumyloxy radicals and c) formation of DCP via recombination of two cumyl peroxy radicals.

Figure 4 illustrates the decomposition of CHP as a function of % CHP remaining. The objective of this experiment is to determine the stability of cumene hydroperoxide under different reaction conditions. In each case, CHP and the catalyst were added to dodecane, a solvent relatively inert towards radical processes.²⁶ As can be seen, in the absence of a catalyst, the percentage of CHP remaining is relatively constant. However, upon addition of either the support alone (TiO₂) or commercial AuNP@TiO₂, CHP is rapidly consumed.

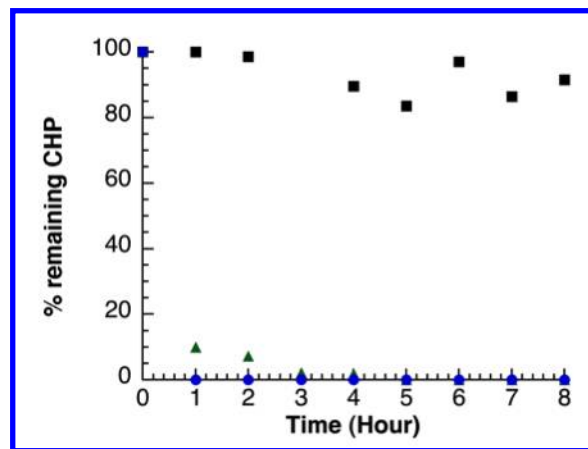


Figure 4. Decomposition of cumene hydroperoxide using no catalyst (■), TiO₂ only (▲) and commercial AuNP@TiO₂ (●) at 80°C.

HPLC analysis of the reaction mixture when TiO₂ alone was used illustrates phenol as the main decomposition product, obtained via an ionic pathway not a free-radical pathway.²⁷ The formation of phenol from CHP is largely dependent on the acidity of the TiO₂. Solomon and Murray²⁸ have shown that hydrated clays (< 6% water content) effectively catalyze the formation of phenol from CHP. When the water content is above this value, no CHP decomposition was observed. Similar experiments were conducted using TiO₂. In one case, the support was calcined at 400°C for 72 hours and in another was used as received. The dried TiO₂ sample rapidly decomposed CHP into phenol at 80°C within 2-3 hours, whereas the hydrated support remained inert toward CHP degradation (Figure S10). The formation of phenol would account for the considerable CHP degradation observed in Figure 3 without detectable amounts of the expected cumyl alcohol free-radical product.

Using AuNP@HT as a catalyst. As shown above, the radical nature of cumene hydroperoxidation ultimately requires that the hydroperoxide must be stable in the presence of the support. Of the other numerous solids tested for inertness toward CHP degradation (*e.g.*, Al₂O₃, ZnO, clays), hydrotalcite (HT; magnesium aluminum anionic clay) was found to meet this criterion and has been shown to be inert towards radical processes.⁵

As shown in Figure 5, though cumyl alcohol is still the major product for the cumene peroxidation reaction using AuNP@HT, a considerable amount of cumene hydroperoxide can be observed after 8 hours of reaction. Control experiments run in the presence of HT only did not show any significant product formation (Figure S10).

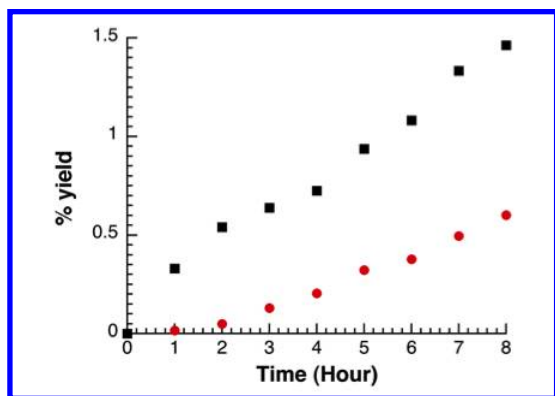


Figure 5. Percent yield of cumyl alcohol (■) and CHP (●) for AuNP@HT catalyzed cumene hydroperoxidation at 80 °C.

The ability of HT and AuNP@HT to degrade cumene hydroperoxide was also assessed (Figure 6). Primarily, in the absence of catalyst or in the presence of HT only, CHP exhibited exceptional stability. However, when AuNP@HT was used as a catalyst, CHP degraded into cumyl alcohol, reaching a plateau after ~2 hours. This plateau is likely due to the fact that the cumene hydroperoxide reagent contains about 20% cumene, which allows for a steady-state to be established between CHP degradation and CHP formation from cumene and atmospheric oxygen in the reaction mixture. When this reaction was carried under inert atmosphere (N₂; Figure S11), complete degradation of the CHP was observed, as the pathway for O₂-facilitated cumene hydroperoxidation was removed. The plateau observed in Figure 6 for AuNP@HT decomposition of CHP could also be partially explained by catalyst fatigue or change in the electronic properties of catalyst. A change in the properties of the catalyst may also be evidenced by the presence of a small induction time observed prior to CHP formation.

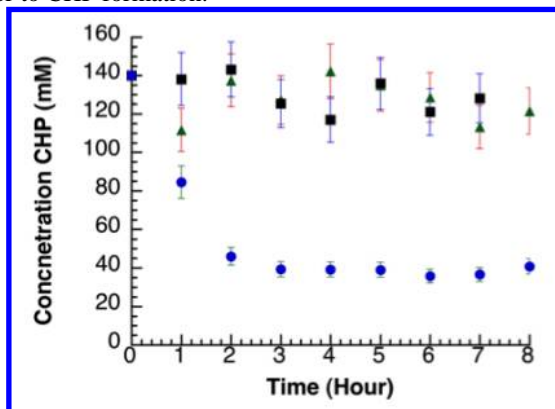


Figure 6. Decomposition of cumene hydroperoxide into cumyl alcohol using no catalyst (■), HT (▲) and AuNP@HT (●) at 80 °C.

The formation and degradation of CHP using commercial AuNP@TiO₂ (Figures 3 and 4) and AuNP@HT (Figures 5 and 6) as catalysts illustrate that AuNP@TiO₂ are more active towards CHP decomposition, whereas AuNP@HT promotes the formation of CHP, the desired precursor of the aforementioned Hock rearrangement. As a nominal 1% Au loading is used for both catalysts, Au concentration must not play a large role in the observed differences in activity between AuNP@TiO₂ and AuNP@HT. The varying results are likely related to the difference in the size of the supported nanopar-

ticles, where smaller particles (and thus more numerous) result in more efficient reaction²⁹ (AuNP@TiO₂ = 2.3 nm; AuNP@HT = 5.8 nm), as well as the effect of the support itself.³⁰

Using AgNP@HT as a catalyst. As HT is relatively inert towards CHP degradation, silver nanoparticles supported on HT (AgNP@HT) were also examined as potential catalysts for cumene peroxidation, as shown in Figure 7, for direct comparison with Au. A considerable increase in the yield of CHP with respect to cumyl alcohol can be observed in the presence of AgNP@HT, as compared with the results obtained using commercial AuNP@TiO₂ and HT (Figures 3 and 5, respectively). The amount of cumyl alcohol obtained when using AgNP@HT is minimal (0.08%) compared to 1.0% for CHP. Moreover, these results suggest very good selectivity toward CHP formation when AgNP@HT are employed as heterogeneous catalyst. The amount of cumyl alcohol obtained in the case of AgNP@HT is minimal and the selectivity toward cumene hydroperoxide is 92 % (after 8 hours of reaction).

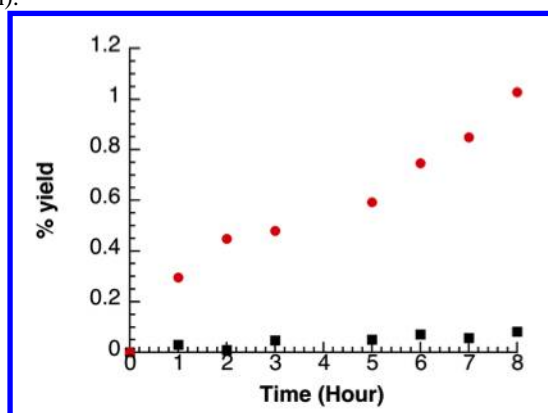


Figure 7. Percent yield of cumyl alcohol (■) and CHP (●) for AgNP@HT catalyzed cumene hydroperoxidation at 80 °C.

Figure 8 illustrates the ability of AgNP@HT to degrade cumene hydroperoxide and shows minimal cumene hydroperoxide degradation (loss of approximately 25% over 8 hours) to cumyl alcohol as compared to AuNP@HT, confirming that CHP is the major product formed when supported AgNP are used as the peroxidation catalyst.

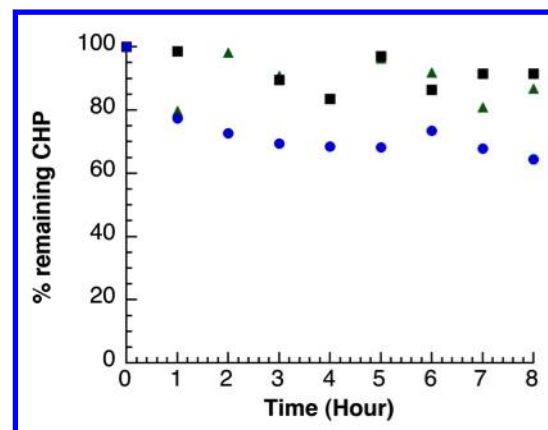


Figure 8. Decomposition of cumene hydroperoxide into cumyl alcohol using no catalyst (■), HT (▲) and AgNP@HT (●) at 80 °C.

In an attempt to increase the overall yield of cumene hydroperoxide formation, the reaction medium was saturated with oxygen (5 mL/min flow). Figure 9 shows that the overall yield of CHP formed after 8 hours of reaction was 9.4% under O₂, as compared to 1.0% under atmospheric conditions. Furthermore, the % yield of cumyl alcohol was also found to increase from 0.08% to 2.4% in the presence of oxygen.

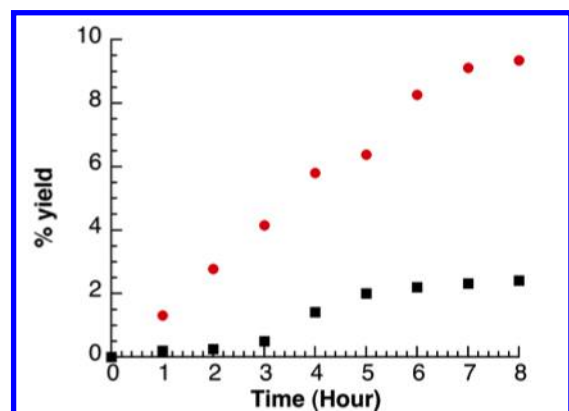


Figure 9. Percent yield of cumyl alcohol (■) and CHP (●) for AgNP@HT catalyzed cumene peroxidation at 80 °C under oxygen saturated conditions.

Table 1 summarizes the % yields of cumyl alcohol and CHP obtained under the different reaction conditions discussed herein, as well towards CHP formation when using supported Au and AgNP as catalysts. Importantly, in the absence of any catalytic material, no significant conversion of cumene to CHP was observed. The reaction was also carried out over a period of 24 hours yielding 18.4 % CHP and 4.8 % cumyl alcohol for a combined conversion of ~25 %. This value is within the range of yields commonly obtained in industry.³¹

Table 1. Product distribution and selectivity of Au and AgNP catalyzed cumene peroxidation after 8 hours reaction at 80 °C.

Catalyst	% Yield Cumyl Alcohol	% Yield CHP	Selectivity CHP (%)
AuNP@HT ^a	0.9	0.3	25 %
AgNP@HT ^a	0.1	1.0	92 %
No catalyst ^a	0.0	0.03	100 %
HT ^a	0.0	0.01	100%
AgNP@HT ^b	2.4	9.4	80%
No catalyst ^b	0	0.1	100%
HT ^b	0.2	1.8	80%

^aAtmospheric conditions

^bOxygen saturated conditions

Recyclability Study

The recyclability of AuNP@HT and AgNP@HT under atmospheric and oxygen saturated conditions are presented in

Figure 10. After AuNP@HT is recycled once, a 2-fold increase in the amount of CHP and a corresponding decrease in the yield of cumyl alcohol was observed. The observed decrease in the obtained yields of cumyl alcohol can be attributed to catalyst fatigue with regards to the efficiency of the material to degrade CHP and can be used to justify the plateau of CHP decomposition observed in Figure 6. When using AgNP@HT as a catalyst under atmospheric conditions, similar yields of CHP and cumyl alcohol are obtained after one reuse, illustrating reasonable stability of the nanocomposite. However, recycling experiments using AgNP@HT under oxygen-saturated conditions illustrate deactivation of the catalyst with respect to both CHP and cumyl alcohol formation. This observation occurs in conjunction with a considerable change in the visual yellow to blue/black. Characterization of the catalyst by TEM analysis shows reduced pore stability of the HT support under these conditions (Figure S12). Notably, TEM images depict the disappearance of the two dimensional, layered structure of the HT. XPS analysis of the supported AgNP (Figure S13) also illustrates some oxidation of the nanoparticles under these reaction conditions.

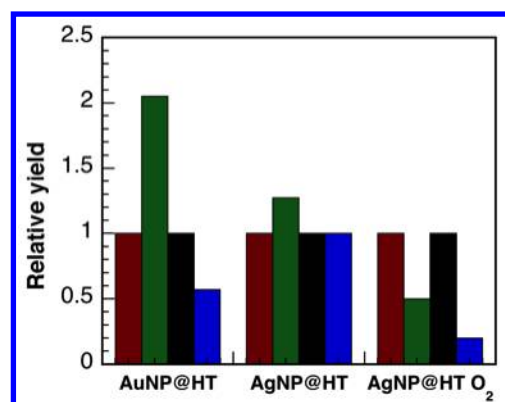


Figure 10. Recyclability experiments after one reuse of AuNP@HT and AgNP@HT (under atmospheric and oxygen saturated conditions): CHP first cycle (■), CHP second cycle (■), cumyl alcohol first cycle (■) cumyl alcohol second cycle (■).

Oxygen Uptake Experiments

The oxygen uptake apparatus was used to evaluate the mechanism of AuNP-mediated cumene peroxidation. This methodology has been widely utilized and is well described in the literature.³² Oxygen uptake kinetics for the free-radical cumene autoxidation is well studied with known rate constants for each elementary step.³³ The purpose of these experiments is to compare cumene peroxidation using supported AuNP with the previously published results for the standard free-radical autoxidation of cumene.

The basic oxygen uptake experiment is described as follows: The oxygen uptake apparatus can be used to determine the rate at which oxygen is consumed by a reaction, effectively probing the propagation step. Figure 11 shows representative data obtained from the oxygen uptake apparatus when monitoring cumene peroxidation, where the slope of the black trace can be used to calculate the rate of propagation, R_p, equivalent to the rate at which oxygen is consumed (see Supporting Information for more details). The red trace represents an experiment where an antioxidant is added to the reaction mixture resulting in an induction period that can be used to determine the rate of initiation (R_i). The antioxidant prevents

the propagation by trapping the radical species that are formed in the initiation step.

Our oxygen uptake apparatus cannot be used at elevated temperatures (maximum 30°C). Under these experimental conditions, AuNP and AgNP@HT showed limited catalytic activity towards the peroxidation process, therefore studies were concentrated on the use of commercial AuNP@TiO₂. Control experiments carried out in the absence of *tert*-butyl hydroperoxide initiator and in the presence of TiO₂ revealed no evidence of oxygen uptake. The rate of oxygen consumption, (R_p) catalyzed by commercial AuNP@TiO₂ experiment was calculated to be $\sim 1.0 \times 10^{-5}$ M/s and decreased as the reaction progressed. The amount of oxygen consumed by the peroxidation reaction was, as expected, equivalent to the sum of cumyl alcohol and cumene hydroperoxide produced (Figure 12).

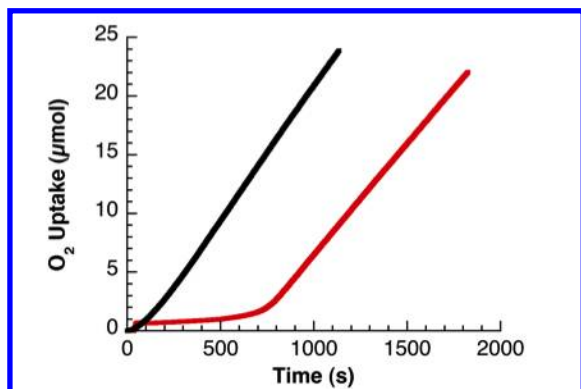


Figure 11. Typical oxygen uptake traces obtained for commercial AuNP@TiO₂-catalyzed cumene peroxidation using *tert*-butyl hydroperoxide as initiator. The black line represents actual experimental data obtained and was used to calculate the amount of O₂ consumed as a function of time and the red line represents actual experimental data using an antioxidant to calculate the rate of initiation.

R_i for cumene peroxidation in the presence of supported AuNP and an antioxidant was also calculated and found to be $\sim 1.7 \times 10^{-7}$ M/s. The equations used for the calculation of R_p and R_i can be found in the Supporting Information. From these values, the average length of the free-radical chain reaction, R_p/R_i , can also be predicted and was determined to be ~ 58 . In principle, this number reflects the ratio between the amount of CHP and cumyl alcohol formed, as CHP is formed in the propagation step and cumyl alcohol is in the initiation step. Thus, R_p/R_i should be proportional to [CHP]/[Cumyl Alcohol].

Aliquots taken from the reaction cells were analyzed *via* HPLC to determine the product distribution ratio obtained from the oxygen uptake experiments (Figure 12). The differences in % yield values shown in this graph as compared to Figure 3 can be attributed to inherent reaction conditions of the oxygen uptake apparatus as compared to those carried out on the bench. These data indicates that the experimental value of [CHP]/[Cumyl Alcohol] is slightly less than 2, clearly lower than the determined free-radical chain length of 58. This discrepancy will be used to further discuss the potential mechanism for AuNP-mediated cumene peroxidation (*vide infra*).

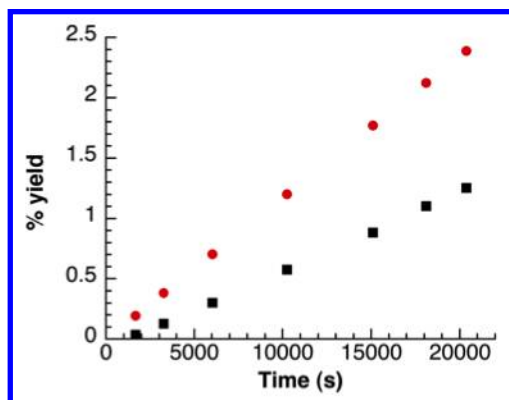


Figure 12. Percent yield of cumyl alcohol (■) and CHP (●) for cumene peroxidation using AuNP@TiO₂ at 30°C using the oxygen uptake technique.

DISCUSSION

Free-radical cumene peroxidation can be described as a typical chain reaction, including initiation, propagation and termination steps. From the results obtained in this work, especially the decomposition of cumene hydroperoxide into cumyl alcohol, it is evident that both AuNP and AgNP have a significant influence on the initiation step. This decomposition can be attributed to a Fenton-like reaction in the presence of metal nanoparticles, as has been previously reported for H₂O₂ decomposition by AgNP³⁴ and also by AuNP supported on nanodiamond.³⁵

As this work was carried out using heterogeneous catalysts, the role of the support must be considered. Previous results obtained for the peroxidation of cyclohexane using various supported AuNP, notably AuNP@TiO₂, attributed the majority of cyclohexane hydroperoxide decomposition to the presence of the nanoparticles.⁸ However, further studies suggested that the support itself could also be responsible for some hydroperoxide decomposition when using Au@nano-CeO₂.¹⁶ In the case of the work discussed herein, the results obtained when using AuNP and AgNP@HT show that the nanoparticles are mainly responsible for the decomposition of CHP into cumyl alcohol. This is evident when HT alone is used as the catalyst and minimal CHP decomposition was observed. However, in experiments where commercial AuNP@TiO₂ was used as a catalyst, the nature (*i.e.*, hydration) of the support played a more important role on CHP stability. Furthermore the major product obtained (phenol) for CHP decomposition when using TiO₂ alone supports an acid-catalyzed mechanism, rather than a free-radical pathway.³⁶

When considering the pathways responsible for supported nanoparticle-catalyzed cumene peroxidation it is important to consider past literature precedents.^{34, 35, 37} Both Au and Ag nanoparticles actively decompose hydroperoxides *via* a Fenton-like reaction. As such, the initial step in our schematic representation, presented in Figure 13, involves adsorption of hydroperoxide (either the *tert*-butyl hydroperoxide initiator or cumene hydroperoxide formed throughout the reaction) onto the NP surface and a subsequent Fenton cleavage to result in RO• and HO⁻. The possibility of a homogeneous catalysis caused by catalytic leaching of supported AuNP into the reaction mixture was also considered, as such a pathway would lead to Fenton chemistry happening in solution. However, no Au could be detected following ICP analysis of the catalytic reaction mixture after the removal of the catalyst by

centrifugation, ruling out such a possibility. Following the initial Fenton cleavage of the hydroperoxide via the adsorption of ROOH onto the nanoparticle surface, the nanoparticle-catalyzed peroxidation of cumene can be thought of as involving a combination of radical reactions occurring in solution and on the nanoparticle surface. The reactions occurring on the nanoparticle surface could influence any of the steps of the free-radical mechanism shown in equations (1)-(4), either while on the surface or through exchange between the surface

and the solution. Only the initiation (reaction 1) is likely unimportant in the solution phase at 80°C, while other steps may be viable in either phase. For example, considering that the reaction rate between carbon-centered radicals and oxygen is close to diffusion-controlled ($10^9 \text{ M}^{-1}\text{s}^{-1}$),³⁸ it would be unlikely for the step involving reaction between the cumyl radical and oxygen to be more efficient on the nanoparticle surface, as it is already the dominant pathway for cumyl radicals.

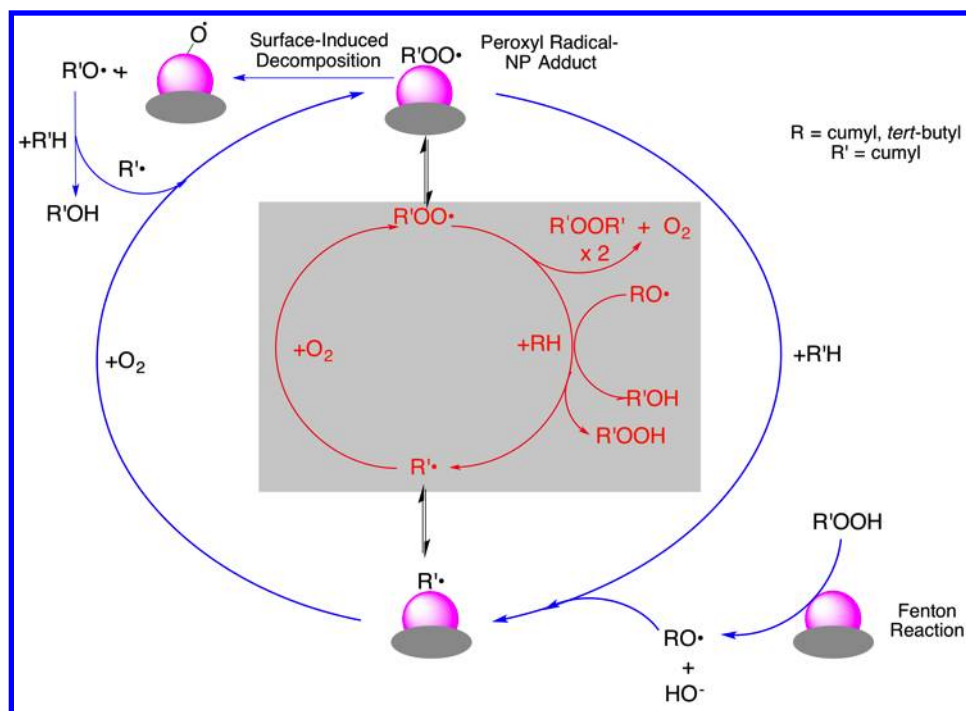


Figure 13. Schematic representation of cumene peroxidation in the presence of metallic nanoparticles. Blue arrows are representative of reactions occurring on the nanoparticle surface, while red arrows indicate pathways within the bulk solution. The red pathway enclosed in a grey box is well established in solution; such homogeneous autooxidation is a slow process at the temperatures used in this work, but this may be largely due to inefficient homogeneous initiation.

In this work and under the presence of oxygen, the radical that interacts with the gold surface is likely an oxygen-centered radical, either alkoxy or peroxy in nature, derived from the cumyl radical. Thus, following formation of $\text{RO}\cdot$ via Fenton chemistry, H-abstraction from a molecule of cumene results in the formation of a cumyl radical and cumyl alcohol. Subsequent reaction between the cumyl radical and O_2 gives rise to cumyl peroxy radicals as the main intermediates. It is important to note that adsorption of oxygen-centered radicals onto the nanoparticle surface is considered a rapid process,³⁹ though competition with the H-abstraction pathway in solution cannot be dismissed. Aprile *et al.* also have suggested the formation of a similar type of peroxy radical-AuNP adduct.⁴⁰

Once formed, the possible fate of the cumyl peroxy radical-nanoparticle adduct is two fold. Firstly, the binding between the nanoparticle surface and the peroxy radical may be reversible and simply go back into solution. This intermediate could then undergo either 1) H-abstraction from an additional molecule of cumene, forming cumene hydroperoxide and cumyl alcohol or 2) a termination step to form dicumyl peroxide (DCP). This is supported by the small amounts of DCP illustrated in Figure 3, when commercial AuNP@TiO₂ are employed as the reaction catalyst and corroborates the presence of a solution-based pathway.

The second possibility involves surface-induced decomposition of the cumyl peroxy radical-nanoparticle adduct (see top-left in Figure 13); this pathway ultimately generates a molecule of cumyl alcohol and a radical $\text{R}\cdot$ that re-enters the autooxidation reaction. Though H-abstraction is still possible to yield CHP, evidence for surface decomposition of methyl peroxy radical-nanoparticle adducts has been previously observed.⁴¹ From the aforementioned findings, O-O bond cleavage is favoured over Au-O dissociation.⁴¹ In the context of Figure 13, this would result in the formation of Au-O• and $\text{RO}\cdot$, yielding cumyl alcohol as the final product. Similar Au-O species have been recently predicted as active participants in the interaction of AuNP with oxygen and hydrocarbons.⁴²

The oxygen uptake experiments can be used to support the formation of cumyl alcohol by a pathway other than the initial hydroperoxide decomposition, as shown to the right of Figure 12. The free-radical chain length was predicted to be ~58. Recalling that this value (R_p/R_i) is proportional to $[\text{CHP}]/[\text{Cumyl Alcohol}]$, if the only mechanism for the formation of cumyl alcohol were nanoparticle-catalyzed CHP decomposition, the calculated $[\text{CHP}]/[\text{Cumyl Alcohol}]$ should be similar to the predicted value. However, the calculated chain length from analysis of HPLC product distribution was ~2. This suggests that the concentration of cumyl alcohol is

considerably larger than originally predicted and indicates that an additional nanoparticle-induced pathway may be responsible for alcohol formation. One such possibility entails the surface induced decomposition of cumyl peroxy radicals. Unfortunately oxygen uptake reactions are limited to 30°C, therefore further experiments were carried out to support the suggested participation of free radicals in solution, as well as nanoparticle surface chemistry in the mechanism presented in Figure 13. 2,6-di-*tert*-butyl-4-methoxyphenol (DBHA) was added one hour after the reaction to trap any free-radical species in solution. For AuNP@HT (Figure S18) and AuNP@TiO₂ (Figure S19), addition of DBHA resulted in the inhibition of the product formation over the remaining course of the experiment. These results demonstrate that, at 80°C, supported AuNP catalyzed cumene peroxidation does involve the participation of solution free-radical species. Lipoic acid was also added as a probe in order to get a better understanding on the involvement of the nanoparticle surface, due to the inherently strong interactions between the AuNP and sulfur.⁴³ Ideally, lipoic acid will interact and cap the AuNP surface preventing the surface decomposition of peroxy radical into the corresponding alkoxy radical and decreasing the yield of cumyl alcohol observed. Figures S21 and S22 show the effects of lipoic acid addition to reactions using AuNP@HT and AuNP@TiO₂ as catalysts, respectively. In both cases, lipoic acid appears to halt and plateau the formation of CHP and cumyl alcohol, thus supporting the role of the gold nanoparticle surface in the formation of cumyl alcohol via peroxy radical surface decomposition. It is important to note that given the known contribution of solution free-radical chemistry within the proposed peroxidation mechanism, a complete prevention of CHP and cumyl alcohol formation is not expected, but more so a plateau of the product yields, as is observed.

AgNP@HT can be suggested to be a superior catalyst as the largest yields of the desired CHP product are obtained when this material is used in the reaction. However, even though both AgNP@HT and AuNP@HT, exhibit cumene peroxidation ability, a generalized comparison between the two should not be made due to the differences in both size and nature of the metal nanoparticles. Unfortunately, oxygen uptake experiments could not be carried out using the AgNP@HT catalyst due to lack of activity under the operation conditions of the instrument (i.e., 30°C). Therefore experiments with DBHA (Figure S20) and lipoic acid (Figure S23) at 80°C, similar to those undertaken on the supported AuNPs, were performed. Addition of DBHA showed a decrease in the yields of both CHP and cumyl alcohol indicating an inhibition of free radical chemistry in solution. Lipoic acid has also demonstrated the ability to protect and cap the AgNP surface.⁴⁴ Addition of lipoic acid to the peroxidation reaction using AgNP@HT as a catalyst resulted in a reduction in CHP and cumyl alcohol formation demonstrating involvement of the AgNP surface in the peroxidation mechanism. Given these results, the formation of a peroxy radical-nanoparticle adduct cannot be dismissed. In principle, the surface decomposition of a peroxy radical-AgNP adduct must be a less favoured pathway or, at least, more reversible when AgNP@HT are used as CHP is the product.

Reflecting on the two questions posed within the introduction, the following statements can be made from the present study. First, when considering the ability of Au and AgNP to decompose hydroperoxides, the HPLC product distribution data clearly show this is the case, where AuNP initiate CHP degradation more rapidly than the corresponding Ag composites.

Specifically, cumyl alcohol was determined to be the major product when supported AuNP were used, while CHP was the major product for the supported AgNP-catalyzed cumene peroxidation reaction.

In regards to the second question posted, both supported Au and AgNP were found to influence the kinetics of the peroxidation reaction. In the absence of supported nanoparticles at 80°C, minimal peroxidation products were observed after 8 hours, but addition of the heterogeneous nanoparticle catalyst increased the yields of both CHP and cumyl alcohol formed with the reaction mixture. The formation of the proposed peroxy radical-nanoparticle adduct would be expected to play an important role in the kinetics of this reaction.

CONCLUSION

Peroxidation of cumene was studied at low conversions due to the interest in understanding the oxidation reaction using supported metal nanoparticles, as this reaction is considerably important from an industrial point of view. Both the role of the support and the nanoparticle were investigated, where the influence of the supported nanoparticles was considerably more important with respect to CHP degradation and cumene peroxidation, than support participation in the reaction. The nature of the supported nanoparticle has a major influence on the overall product distribution, with supported AuNP yielding cumyl alcohol as the major product, and CHP when supported AgNP were used. The data when using supported AuNP, the cumyl alcohol product may have two origins, one through Fenton-induced decomposition of hydroperoxides and a second through surface-induced decomposition of a proposed peroxy radical-nanoparticle adduct.

ASSOCIATED CONTENT

Supporting Information. TEM data for AuNP and AgNP@HT, representative HPLC data, kinetics for cumene peroxidation control experiments, kinetics for CHP decomposition data using hydrated and dried TiO₂ P25, kinetics for CHP decomposition under N₂ using AuNP@HT, description of oxygen uptake apparatus and methodology used for data interpretation.

AUTHOR INFORMATION

Corresponding Authors

*E-mail scaiano@photo.chem.uottawa.ca (JCS), josecarlos@photo.chem.uottawa.ca (JCN-F).

ACKNOWLEDGMENT

We gratefully acknowledge the Natural Sciences and Engineering Research Council of Canada for support of this research. COLC also thanks the government of Ontario for an OGS scholarship. JCN-F thanks the University of Ottawa for a visiting professor fellowship. M. G. B. also thanks the Spanish Ministry of Economy and Competitiveness for her Juan de la Cierva contract and FP7-PEOPLE-2011-CIG (NANOPHOCAT) for financial support.

REFERENCES

1. Weissmehl, K.; Arpe, K. J., *Industrial Organic Chemistry*, 4th Edition. Wiley-VCH Darmstadt, Germany, 2003.
2. Kamir, Y.; Beaton, S.; Lafortune, A.; Ingold, K. U., *The Metal-Catalyzed Autooxidation of Tetralin: I. Introduction. The Cobalt-Catalyzed Autooxidation in Acetic Acid*. *Can. J. Chem.* 1963, 41, 2020-2033.

3. Woodward, A.; Mesrobian, R. B., Low Temperature Autoxidation of Hydrocarbons. The Kinetics of Tetralin Oxidation. *J. Am. Chem. Soc.* 1953, 75, 6189-6195.
4. Varma, G. R.; Graydon, W. F., Heterogeneous Catalytic Oxidation of Cumene (Isopropyl Benzene) in Liquid Phase. *J. Catal.* 1973, 28, 236-244.
5. Jana, S. K.; Wub, P.; Tatsumi, T., NiAl Hydrotalcite as an Efficient and Environmentally Friendly Solid Catalyst for Solvent-Free Liquid-Phase Selective Oxidation of Ethylbenzene to Acetophenone with 1 atm of Molecular Oxygen. *J. Catal.* 2006, 240, 268-274.
6. Casemier, J. H. R.; Nieuwenhuys, B. E.; Sachlter, W. M. H., The Oxidation of Cumene and the Decomposition of Cumene Hydroperoxide on Silver, Copper and Platinum. *J. Catal.* 1973, 29, 367-373.
7. Richardson, W. H., Metal Ion Decomposition of Hydroperoxides. II. Kinetics and Mechanism of Cobalt Salt Catalyzed Decomposition of t-Butyl Hydroperoxide. *J. Am. Chem. Soc.* 1965, 87, 1096-1102.
8. Hereijgers, B. P. C.; Weckhuysen, P. M., Aerobic Oxidation of Cyclohexane by Gold-Based Catalysts: New Mechanistic Insight by Thorough Product Analysis. *J. Catal.* 2010, 210, 16-25.
9. Xu, Y. J.; Landon, P.; Enache, D.; Carley, A. F.; Roberts, M. W.; Hutchings, G. J., Selective Conversion of Cyclohexane to Cyclohexanol and Cyclohexanone using a Gold Catalyst under Mild Conditions. *Cat. Lett.* 2005, 101, 175-179.
10. Liu, Y.; Tsunoyama, H.; Akita, T.; Xie, S.; Tsukuda, T., Aerobic Oxidation of Cyclohexane Catalyzed by Size-Controlled Au Clusters on Hydroxyapatite: Size Effect in the Sub-2 nm Regime. *ACS Catal.* 2011, 1, 2-6.
11. Zhoua, H. J.; Luoa, H.; Zenga, C.; Lia, D.; Liu, Y., Synthesis, Characterization of Ag/MCM-41 and the Catalytic Performance for Liquid-Phase Oxidation of Cyclohexane. *Cat. Lett.* 2006, 108, 49-55.
12. Centi, G.; Perathoner, S.; Trifiro, F., Sustainable Industrial Chemistry. Wiley-VCH: Weinheim, Germany, 2009.
13. Van Ham, N. H. A.; Nieuwenhuys, B. E.; Sachtler, W. M. H., The Oxidation of Cumene on Silver and Silver-Gold Alloys. *J. Catal.* 1971, 20, 408-423.
14. Panayotava, E. N.; Dimitrov, D. I.; Petkov, A. A., On the Role of Metallic Copper in the Oxidation of Cumene to Cumene Hydroperoxide. *J. Catal.* 1976, 41, 329-332.
15. Zu, S.; Hang, C.; Zhang, J.; Chen, B., Catalytic Activity of Cu/MgO in Liquid Oxidation of Cumene. *Korean J. Chem. Eng.* 2009, 26, 1568-1573.
16. Lloyd, R.; Jenkins, R. L.; Piccinini, M.; He, Q.; Kiely, C. J.; Golunski, S. E.; Bethell, D.; Bartley, J. K.; Hutchings, G. J., Low-temperature aerobic oxidation of decane using an oxygen-free radical initiator. *J. Catal.* 2011, 283, 161-167.
17. Goszner, K.; Bischof, N., The Decomposition of Hydrogen Peroxide on Silver-Gold Alloys. *J. Catal.* 1974, 32, 175-182.
18. Navalon, S.; de Miguel, M.; Martin, R.; Alvaro, M.; Garcia, H., Enhancement of the Catalytic Activity of Supported Gold Nanoparticles for the Fenton Reaction by Light. *J. Am. Chem. Soc.* 2011, 133, 2218-2226.
19. Schmidt, R. J., Industrial Catalytic Processes - Phenol Production. *Appl. Catal. A: General* 2005, 280, 89-103.
20. Mitsudome, T.; Noujima, A.; Mizugaki, T.; Jitsukawa, K.; Kaneda, K., Efficient Aerobic Oxidation of Alcohols using a Hydrotalcite-Supported Gold Nanoparticle Catalyst. *Adv. Synth. Catal.* 2009, 351, 1890-1896.
21. Mitsudome, T.; Mikami, Y.; Funai, H.; Mizugaki, T.; Jitsukawa, K.; Kaneda, K., Supported Silver-Nanoparticle-Catalyzed Highly Efficient Aqueous Oxidation of Phenylsilanes to Silanols. *Angew. Chem. Int. Ed.* 2008, 47, 138-141.
22. Howard, J. A., *Advances in Free Radical Chemistry, Volume 4*. Logos Press: London, England, 1972.
23. Fillippenko, V. University of Ottawa, MSc Thesis: Oxygen Uptake Studies of Organic and Inorganics Oxidations, 2010.
24. Barclay, L. R. C.; Vinqvist, M. R., Membrane Peroxidation: Inhibiting Effects of Water Soluble Antioxidants on Phospholipids of Different Charge Types. *Free Radic. Biol. Med.* 1994, 16, 779-788.
25. Kharasch, M. S.; Fono, A.; Nudernberg, W., The Chemistry of Hydroperoxide III. The Free-Radical Decomposition of Hydroperoxides. *J. Org. Chem.* 1949, 763-774.
26. Barrett, K. E.; Thomas, H. R., Kinetics of Dispersion Polymerization of Soluble Monomers. I. Methyl Methacrylate. *J. Polym. Sci. Pol. Chem.* 1969, 7, 2621-2650.
27. Kharasch, M. S.; Fono, A.; Nuderberg, W., The chemistry of Hydroperoxides I. The acid-catalysed Decomposition of alpha,alpha-Dimethylbenzyl (alpha-Cumyl) Hydroperoxide. *J. Org. Chem.* 1949, 748-752.
28. Solomon, D. H.; Murray, H. M., Acid-Base Interactions and the Properties of Kaolinite in Non-Aqueous Media. *Clays and Clays Miner.* 1972, 20, 135-141.
29. Corma, A.; Garcia, H., Supported gold nanoparticles as catalysts for organic reactions. *Chem. Soc. Rev.* 2008, 37, (9), 2096-2126.
30. Naya, S.-i.; Teranishi, M.; Kimurab, K.; Tada, H., A strong support-effect on the catalytic activity of gold nanoparticles for hydrogen peroxide decomposition. *Chem. Commun.* 2011, 47, 3230-3232.
31. Chauvel, A.; Lefebvre, G. G., *Petrochemical Processes: Technical and Economic Characteristic*. Ophrys: Paris, 1989; Vol. 2.
32. Barclay, L. R. C.; Ingold, K. U., Autoxidation of biological molecules. 2. Autoxidation of a model membrane. Comparison of the autoxidation of egg lecithin phosphatidylcholine in water and in chlorobenzene. *J. Am. Chem. Soc.* 1981, 103, (21), 6478-6485.
33. Howard, J. A.; Ingold, K. U., Absolute Rate Constants for Hydrocarbon Oxidation. XI. The Reactions of Tertiary Peroxy Radicals. *Can. J. Chem.* 1968, 46, 2555-2660.
34. Jones, A. M.; Garg, S.; He, D.; Pham, A. N.; Waite, T. D., Superoxide-Mediated Formation and Charging of Silver Nanoparticles. *Environ. Sci. Technol.* 2011, 45, 1428-1434.
35. Navalon, S.; Martin, R.; Alvaro, M.; Garcia, H., Gold on Diamond Nanoparticles as a Highly Efficient Fenton Catalyst. *Angew. Chem. Int. Ed.* 2010, 49, 8403-8407.
36. Salukvadze, L. V.; Norikov, Y. D.; Valendo, A. Y.; Blyumberg, E. A., The Oxidation of Cumene in the Presence of Heterogenous Oxide Catalysts in the Liquid Phase. *Russ. Chem. Bull.* 1972, 7, 1478-1482.
37. Della Pina, C.; Falletta, E.; Prati, L.; Rossi, M., Selective oxidation using gold. *Chem. Soc. Rev.* 2008, 37, (9), 2077-2095.
38. Maillard, B.; Ingold, K. U.; Scaiano, J. C., Rate Constants for the Reactions of Free Radicals with Oxygen in Solution. *J. Am. Chem. Soc.* 1983, 105, 5095-5099.
39. Menchon, C.; Martin, R.; Apostolova, N.; Victor, V. M.; Alvaro, M.; Herance, J. R.; Garcia, H., Gold Nanoparticles Supported on Nanoparticulate Ceria as a Powerful Agent against Intracellular Oxidative Stress. *Small* 2012, 8, 1895-1903.
40. Aprile, C.; Corma, A.; Domine, M. E.; Garcia, H.; Mitchell, C., A Cascade Aerobic Epoxidation of Alkenes over Au/CeO₂ and Ti-mesoporous Material by "In Situ" Formed Peroxides. *J. Catal.* 2009, 264, 44-53.
41. Bar-Ziv, R.; Zilbermann, I.; Zidki, T.; Cohen, H.; Meyerstein, D., Reactions of Alkyl Peroxyl Radicals with Metal Nanoparticles in Aqueous Solutions. *J. Phys. Chem. C.* 2009, 113, 3281-3286.
42. Boronat, M.; Corma, A., Molecular approaches to catalysis: Naked gold nanoparticles as quasi-molecular catalysts for green processes. *J. Catal.* 2011, 284, (2), 138-147.

- 1 43. Brust, M.; Walker, M.; Bethell, D.; Schiffrin, D. J.;
2 Whyman, R., Synthesis of Thiol-derivatised Gold Nanoparticle in
3 a Two-Phase Liquid-Liquid System. *J. Chem. Soc., Chem.*
4 *Commun.* 1994, 801-802.
5 44. Gan, W.; Xu, B.; Dai, H. L., Activation of Thiols at a
6 Silver Nanoparticle Surface. *Angew. Chem. Int. Ed.* 2011, 50,
7 6622-6625.
8
9
10
11
12
13
14
15
16
17
18
19
20
21
22
23
24
25
26
27
28
29
30
31
32
33
34
35
36
37
38
39
40
41
42
43
44
45
46
47
48
49
50
51
52
53
54
55
56
57
58
59
60

TOC graphic

